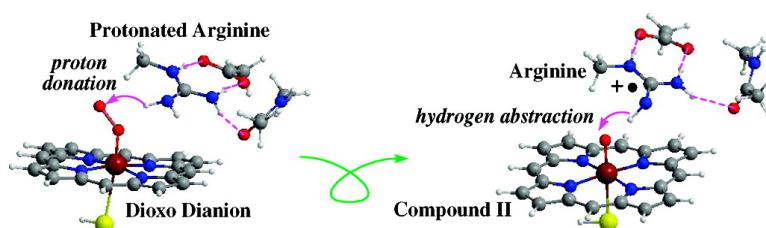Article

Is the Bound Substrate in Nitric Oxide Synthase Protonated or Neutral and What Is the Active Oxidant that Performs Substrate Hydroxylation?

Sam P. de Visser, and Lee Siew Tan

More About This Article

Additional resources and features associated with this article are available within the HTML version:

- Supporting Information
- Links to the 1 articles that cite this article, as of the time of this article download
- Access to high resolution figures
- Links to articles and content related to this article
- Copyright permission to reproduce figures and/or text from this article

View the Full Text HTML

Is the Bound Substrate in Nitric Oxide Synthase Protonated or Neutral and What Is the Active Oxidant that Performs Substrate Hydroxylation?

Sam P. de Visser* and Lee Siew Tan

Manchester Interdisciplinary Biocenter and the School of Chemical Engineering and Analytical Science, The University of Manchester, 131 Princess Street, Manchester, M1 7DN, United Kingdom

Received February 13, 2008; E-mail: sam.devisser@manchester.ac.uk

Abstract: We present here results of a series of density functional theory (DFT) studies on enzyme active site models of nitric oxide synthase (NOS) and address the key steps in the catalytic cycle whereby the substrate (L-arginine) is hydroxylated to N^ω-hydroxo-arginine. It has been proposed that the mechanism follows a cytochrome P450-type catalytic cycle; however, our calculations find an alternative low energy pathway whereby the bound L-arginine substrate has two important functions in the catalytic cycle, *namely first as a proton donor and later as the substrate in the reaction mechanism*. Thus, the DFT studies show that the oxo-iron active species (compound I) cannot abstract a proton and neither a hydrogen atom from protonated L-arginine due to the strength of the N—H bonds of the substrate. However, the hydroxylation of neutral arginine by compound I and its one electron reduced form (compound II) requires much lower barriers and is highly exothermic. Detailed analysis of proton transfer mechanisms shows that the basicity of the dioxo dianion and the hydroperoxo-iron (compound 0) intermediates in the catalytic cycle are larger than that of arginine, which makes it likely that protonated arginine donates one of the two protons needed during the first catalytic cycle of NOS. Therefore, DFT predicts that in NOS enzymes arginine binds to the active site in its protonated form, but is deprotonated during the oxygen activation process in the catalytic cycle by either the dioxo dianion species or compound 0. As a result of the low ionization potential of neutral arginine, the actual hydroxylation reaction starts with an initial electron transfer from the substrate to compound I to create compound II followed by a concerted hydrogen abstraction/radical rebound from the substrate. These studies indicate that compound II is the actual oxidant in NOS enzymes that performs the hydroxylation reaction of arginine, which is in sharp contrast with the cytochromes P450 where compound II was shown to be a sluggish oxidant. This is the first example of an enzyme where compound II is able to participate in the reaction mechanism. Moreover, arginine hydroxylation by NOS enzymes is catalyzed in a significantly different way from the cytochromes P450 although the active sites of the two enzyme classes are very similar in structure. Detailed studies of environmental effects on the reaction mechanism show that environmental perturbations as appear in the protein have little effect and do not change the energies of the reaction. Finally, a valence bond curve crossing model has been set up to explain the obtained reaction mechanisms for the hydrogen abstraction processes in P450 and NOS enzymes.

Introduction

Nitric oxide (NO) is a highly reactive molecule and therefore in biosystems it has to be synthesized close to the source where it is needed. NO functions as a messenger molecule in the brain and is involved in blood pressure control and heart rate.[1−4] The biosynthesis of NO in the body is performed by the heme-enzyme nitric oxide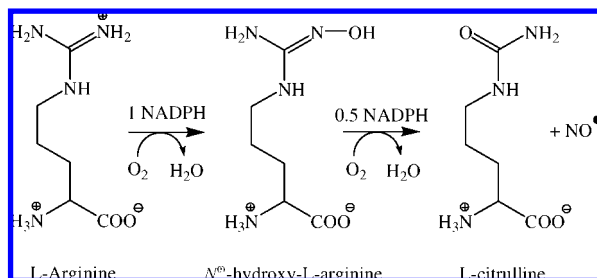 synthase (NOS), which is an important enzyme in human physiology, and understanding its mechanism will help identify suitable inhibitors. Stimulating NOS enzymes with inhibitors by pharmacological or gene therapies effects inflammatory disorders, cardiovascular diseases, pain, and neuroprotection.[5] Moreover, NOS inhibition has been implicated with effects on Parkinson's disease, Alzheimer's disease, epilepsy, and stroke.[6]

NOS is a heme-enzyme that binds L-arginine and catalyzes the two-step oxidation (see Scheme 1) to form NO and L-citrulline via the N^ω-hydroxy-L-arginine intermediate.[7] The first step in the reaction is similar to that catalyzed by the

(1) (a) Murad, F. *Angew. Chem., Int. Ed.* **1999**, *38*, 1856–1868. (b) Furchgott, R. F. *Angew. Chem., Int. Ed.* **1999**, *38*, 1870–1880. (c) Ignarro, L. J. *Angew. Chem., Int. Ed.* **1999**, *38*, 1882–1892.
(2) (a) Groves, J. T.; Wang, C. C.-Y. *Curr. Opin. Chem. Biol.* **2000**, *4*, 687–695. (b) Poulos, T. L.; Li, H.; Raman, C. S.; Schuller, D. J. *Adv. Inorg. Chem.* **2000**, *51*, 243–294. (c) Rousseau, D. L.; Li, D.; Couture, M.; Yeh, S.-R. *J. Inorg. Biochem.* **2005**, *99*, 306–323.
(3) (a) Stuehr, D. J.; Santolini, J.; Wang, Z.-Q.; Wei, C.-C.; Adak, S. *J. Biol. Chem.* **2004**, *279*, 36167–36170. (b) Stuehr, D. J.; Wei, C.-C.; Wang, Z.; Hille, R. *Dalton Trans.* **2005**, 3427–3435.
(4) Marletta, M. A. *Cell* **1994**, *78*, 927–930.
(5) Bredt, D. S.; Snyder, S. H. *Annu. Rev. Biochem.* **1994**, *63*, 175–195.
(6) (a) Nathan, C.; Xie, Q.-W. *Cell* **1994**, *78*, 915–918. (b) Schmidt, H. H. H. W.; Walter, U. *Cell* **1994**, *78*, 919–925. (c) Colton, C. A.; Vitek, M. P.; Wink, D. A.; Xu, Q.; Cantillana, V.; Previti, M. L.; Van Nostrand, W. E.; Weinberg, B.; Dawson, H. *Proc. Natl. Acad. Sci. U.S.A.* **2006**, *103*, 12867–12872.

Scheme 1. Conversion of L-Arginine into L-Citrulline and NO as Catalyzed by NOS Enzymes

Scheme 2. Schematic Drawing of the Active Site of Nitric Oxide Synthase as Taken from the 4NSE pdb File[11][a]

[a] Substrate arginine is bound and held in position with hydrogen bonds with Glu_{363} and Trp_{358} as indicated. Labels taken from the pdb file.

cytochromes P450 (P450) and requires one molecule of oxygen and two electrons.[8] The second step, by contrast, uses only one electron but still one molecule of molecular oxygen. It has been suggested therefore that both reactions are catalyzed by different catalytic cycles and maybe even by different oxidants.[9]

There are three major NOS isoforms—the neuronal (nNOS), endothelial (eNOS), and cytokine inducible (iNOS) enzymes, which are distinguished by their sequence, tissue location, regulation, and catalytic activities.[2,3,10] Each NOS isozyme contains an oxygenase domain that binds iron protoporphyrin IX (heme), tetrahydrobiopterin (H_4B), and arginine.[7] NOS enzymes bind molecular oxygen to the heme iron and convert it during their catalytic cycle into an oxo-iron species that catalyzes the arginine oxidation. However, the latter stages of the catalytic cycle of NOS are sufficiently fast that thus far the active species has not been detected and the catalytic mechanism therefore is mainly based on speculation.

Scheme 2 shows an extract from a crystal structure of the active site of NOS as taken from the 4NSE pdb file.[11] The active center contains a heme group of which the metal is bound to the peptide backbone via a thiolate bridge of a cysteinate residue (Cys_{186}), which is the axial ligand. This catalytic center closely resembles the active site structure of other heme enzymes, such as the P450s.[12] The sixth ligand site of iron (the distal site) is vacant in the pdb file but nearby L-arginine (the substrate) is bound. The guanidinium group of L-arginine forms a salt bridge with the carboxylic acid side chain of Glu_{363} and is also in hydrogen-bonding distance with the peptide carbonyl group between Trp_{358} and Tyr_{359} as indicated in Scheme 2. It has been anticipated that molecular oxygen will bind to the distal site and that L-arginine is converted into N^{ω}-hydroxy-arginine via
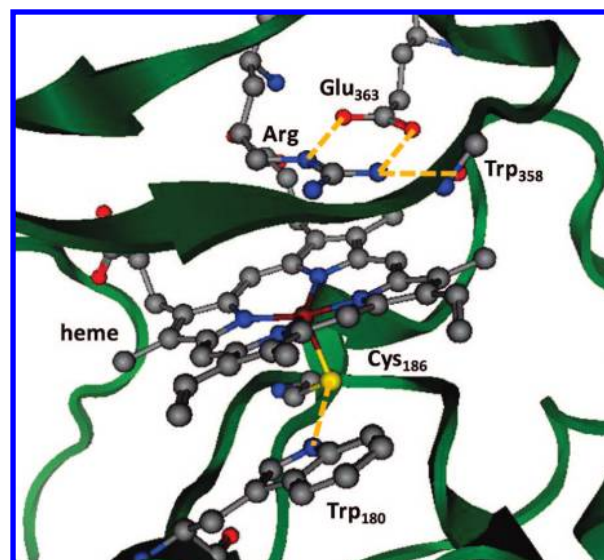
a monooxygenase reaction. In a subsequent reaction with another molecule of oxygen this intermediate is transformed into L-citrulline and NO. The focus of this paper, however, will be on the first step in the reaction mechanism, namely the hydroxylation of L-arginine.

NOS enzymes undergo a complicated catalytic cycle that starts with substrate binding followed by reduction of the heme and binding of molecular oxygen to the heme. A further reduction and two protonation steps convert the system into an oxo-iron species (compound I, CpdI), which has been proposed to be the active species of this enzyme.[7] Despite many efforts in the field the oxo-iron active species of NOS enzymes has never been detected and the mechanism of L-arginine oxidation is surrounded by controversies. Detailed low-temperature studies of eNOS characterized a peroxo-iron complex with EPR/ENDOR and resonance Raman spectroscopy.[13] However, these studies failed to characterize subsequent species in the catalytic cycle such as the hydroperoxo-iron complex (compound 0, Cpd0) and CpdI. The authors, therefore, suggested that the arginine substrate may donate a proton in the catalytic cycle of NOS presumably the second one.[13a] The neutral substrate then is either hydroxylated by CpdI directly or transfers an electron to form compound II prior to the hydroxylation event.[9] To gain insight into the catalytic mechanism of L-arginine hydroxylation by NOS enzymes we have performed a series of density functional theoretic calculations on an active site model of NOS. In this work we address whether the substrate is protonated or neutral in the binding pocket and the mechanism of hydroxylation. Notwithstanding the many density functional theory (DFT) studies on the catalytic cycle and substrate oxidation of P450 enzymes,[14] surprisingly the work done on NOS enzymes

(7) (a) Griffith, O. W.; Stuehr, D. J. *Annu. Rev. Physiol.* **1995**, *57*, 707–736. (b) Wei, C.-C.; Crane, B. R.; Stuehr, D. J. *Chem. Rev.* **2003**, *103*, 2365–2383.

(8) (a) Sono, M.; Roach, M. P.; Coulter, E. D.; Dawson, J. H. *Chem. Rev.* **1996**, *96*, 2841–2888. (b) Kadish, K. M., Smith, K. M., Guilard, R., Eds. *The Porphyrin Handbook*; Academic Press: San Diego, CA, 2000. (c) Groves, J. T. *Proc. Natl. Acad. Sci. U.S.A.* **2003**, *100*, 3569–3574. (d) Guengerich, F. P. *Chem. Res. Toxicol.* **2001**, *14*, 611–650. (e) Ortiz de Montellano, P. R., Ed. *Cytochrome P450: Structure, Mechanism and Biochemistry*, 3rd ed.; Kluwer Academic/Plenum Publishers: New York, 2004.

(9) Rosen, G. M.; Tsai, P.; Pou, S. *Chem. Rev.* **2002**, *102*, 1191–1199.

(10) (a) Li, H.; Flinspach, M. L.; Igarashi, J.; Jamal, J.; Yang, W.; Gómez-Vidal, J. A.; Litzinger, E. A.; Huang, H.; Erdal, E. P.; Silverman, R. B.; Poulos, T. L. *Biochemistry* **2005**, *44*, 15222–15229. (b) Dunford, A. J.; Rigby, S. E. J.; Hay, S.; Munro, A. W.; Scrutton, N. S. *Biochemistry* **2007**, *46*, 5018–5029.

(11) Raman, C. S.; Li, H.; Martásek, P.; Král, V.; Masters, B. S. S.; Poulos, T. L. *Cell* **1998**, *95*, 939–950.

(12) (a) Poulos, T. L.; Finzel, B. C.; Howard, A. J. *Biochemistry* **1986**, *25*, 5314–5322. (b) Schlichting, I.; Berendzen, J.; Chu, K.; Stock, A. M.; Maves, S. A.; Benson, D. E.; Sweet, R. M.; Ringe, D.; Petsko, G. A.; Sligar, S. G. *Science* **2000**, *287*, 1615–1622.

(13) (a) Davydov, R.; Ledbetter-Rogers, A.; Martásek, P.; Larukhin, M.; Sono, M.; Dawson, J. H.; Masters, B. S. S.; Hoffman, B. M. *Biochemistry* **2002**, *41*, 10375–10381. (b) Chartier, F. J. M.; Blais, S. P.; Couture, M. *J. Biol. Chem.* **2006**, *281*, 9953–9962. (c) Chartier, F. J. M.; Couture, M. *J. Biol. Chem.* **2007**, *282*, 20877–20886.

(14) (a) Loew, G. H.; Harris, D. L. *Chem. Rev.* **2000**, *100*, 407–419. (b) Harris, D. L. *Curr. Opin. Chem. Biol.* **2001**, *5*, 724–735. (c) Meunier, B.; de Visser, S. P.; Shaik, S. *Chem. Rev.* **2004**, *104*, 3947–3980.

is sparse. Cho and Gauld[15] presented theoretical studies on the second step in Scheme 1 above that addressed the dioxygen binding step, in particular with respect to its interaction with N^ω-hydroxo-arginine and the reaction leading to L-citrulline and NO. Quantum mechanics/molecular mechanics (QM/MM) studies highlighted the importance of hydrogen bonding toward the thiolate ligand for structures with NO bound.[16] The only study on the first step of the NO biosynthesis of Scheme 1 is a QM/MM study of Shaik et al.[17] that focused on the electronic properties of CpdI and described possible proton transfer mechanisms in the catalytic cycle leading to its formation. The questions that remain, however, are what is the substrate that is hydroxylated by the oxo-iron species? Is there a possibility that arginine, although bound in its protonated form, can donate a proton in the catalytic cycle? Is it really CpdI that is the actual catalyst in NOS enzymes or is an alternative oxidant masquerading as CpdI-like activity? The present paper will try to answer these questions through detailed DFT calculations on model complexes. As will be shown in this work, the substrate in NOS enzymes has a dual role, namely, it acts as a proton donor in the catalytic cycle and as the substrate in a later step. These two functions are intertwined and make the enzyme work.

Methods

Our procedures are similar to previous calculations in the field which we will briefly summarize here.[18] We used the unrestricted hybrid density functional method UB3LYP in combination with a double-ζ quality LACVP basis set on iron and 6−31G on the rest of the atoms (basis set B1).[19] Full optimizations were performed in the *Jaguar 7.0* program package and a subsequent analytical frequency in Gaussian 03 was done.[20,21] To improve the energetics, single point calculations with a triple-ζ quality basis set on Fe (LACV3P+) and 6−311+G* on the rest of the atoms were performed (basis set B2). Energies reported in this work are all $\Delta E + ZPE$ values with energies using basis set B2 and zero-point energy with basis set B1. All local minima described here had real frequencies only, while the transition states are characterized by a single imaginary frequency for the correct mode.

Our model was based on the active site of the 4NSE pdb.[11] We used an active site model where the heme is replaced with protoporphyrin IX (without side chains), abbreviated the axial cysteinate ligand (Cys$_{186}$) with thiolate, and used methylguanidinium for L-arginine. As the substrate is held in position via several strong hydrogen-bonding interactions within the active site pocket, the side chain of Glu$_{363}$ is included in the model with an acetate group, whereas part of the peptide bond between Trp$_{358}$ and Tyr$_{359}$ is also incorporated, see Scheme 3. To prevent these groups from undergoing large and unnatural changes with respect to the crystal structure, the aliphatic carbon atom of Glu$_{363}$ and the two terminating carbon atoms of the peptide chain between Trp$_{358}$ and Tyr$_{359}$ were constrained with respect to the iron heme. The characteristic features of the model are shown in Scheme 3. The first model (model A)

(15) (a) Cho, K.-B.; Gauld, J. W. *J. Am. Chem. Soc.* **2004**, *127*, 10267–10270. (b) Cho, K.-B.; Gauld, J. W. *J. Phys. Chem. B* **2005**, *109*, 23706–23714.

(16) Fernández, M. L.; Martí, M. A.; Crespo, A.; Estrin, D. A. *J. Biol. Inorg. Chem.* **2005**, *10*, 595–604.

(17) Cho, K.-B.; Derat, E.; Shaik, S. *J. Am. Chem. Soc.* **2007**, *129*, 3182–3188.

(18) (a) de Visser, S. P. *J. Am. Chem. Soc.* **2006**, *128*, 9813–9824. (b) de Visser, S. P. *J. Am. Chem. Soc.* **2006**, *128*, 15809–15818. (c) Aluri, S.; de Visser, S. P. *J. Am. Chem. Soc.* **2007**, *129*, 14846–14847.

(19) (a) Becke, A. D. *J. Chem. Phys.* **1993**, *98*, 5648–5652. (b) Lee, C.; Yang, W.; Parr, R. G. *Phys. Rev. B* **1988**, *37*, 785–789. (c) Hay, P. J.; Wadt, W. R. *J. Chem. Phys.* **1985**, *82*, 270–283.

(20) *Jaguar 7.0*; Schrödinger, LLC.: Portland, OR, 2007.

(21) Frisch, M. J.; et al. *Gaussian-03*; Gaussian, Inc.: Wallingford, PA, 2003.

Scheme 3. Schematic Drawing of the Model of the Active Site of Nitric Oxide Synthase CpdI as Studied in This Work[a]
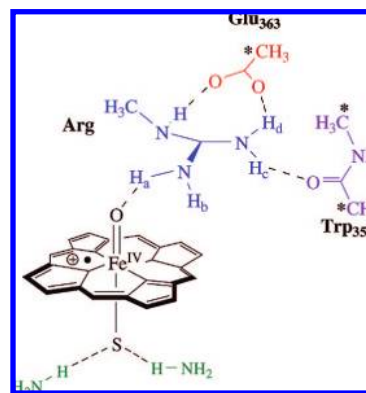
[a] Model A contains protonated L-arginine, in model B atom H$_b$ is removed, and in model C atom H$_d$ is missing. Atoms labeled with a star were constrained with respect to the heme. Additional calculations had two hydrogen-bonded ammonia molecules mimicking the interactions in the protein.

contains protonated arginine and has overall neutral charge. Subsequently, we tested two deprotonated models, whereby either proton H$_b$ (model B) or H$_d$ (model C) is removed. The model is identified in the label with a subscript and the spin multiplicity with a superscript, i.e. ^{4}CpdI$_A$ is the quartet spin state of CpdI of model A.

As can be seen in Scheme 2 the thiolate ligand of Cys$_{186}$ undergoes hydrogen-bonding interactions with the Trp$_{180}$ residue. To test the effect of these interactions on the relative energies, we ran additional calculations with two extra ammonia molecules hydrogen-bonded to the thiolate mimicking the hydrogen-bonding interactions in the enzyme; these structures are identified with "·2NH$_3$" after the label.[22] In the past we showed that these hydrogen-bonding interactions can influence the polarity of the oxo-iron group and determine regio- and chemoselectivities.[23] Moreover, experimental work on the push-effect of the thiolate ligand in NOS enzymes showed this to be a key interaction.[24] Initially, the coordinates of the ammonia molecules were taken from the literature with a fixed S-HNH$_2$ distance of 2.66 Å and the structures were not reoptimized.[22] These calculations reproduced the energetics of the reaction mechanisms closely but corrected the charge and group spin densities. Subsequently, we did additional calculations where the structures of ^{4}CpdI$_A$·2NH$_3$ and ^{4}CpdI$_B$·2NH$_3$ were fully optimized. As will be shown below, hydrogen-bonding interactions to the thiolate ligand have little effect on reaction energies and reproduce the conclusions of the gas-phase models.

Results

Molecular Orbitals of CpdI. The oxo-iron active species of NOS enzymes is called Compound I (CpdI) and is the elusive oxidant that has never been detected. In analogous enzymes, such as peroxidases and catalases crystallographic and spectroscopic evidence of an oxo-iron species was found and

(22) (a) Ogliaro, F.; Cohen, S.; de Visser, S. P.; Shaik, S. *J. Am. Chem. Soc.* **2000**, *122*, 12892–12893. (b) de Visser, S. P.; Shaik, S.; Sharma, P. K.; Kumar, D.; Thiel, W. *J. Am. Chem. Soc.* **2003**, *125*, 15779–15788.

(23) (a) de Visser, S. P.; Ogliaro, F.; Sharma, P. K.; Shaik, S. *Angew. Chem., Int. Ed.* **2002**, *41*, 1947–1951. (b) de Visser, S. P.; Ogliaro, F.; Sharma, P. K.; Shaik, S. *J. Am. Chem. Soc.* **2002**, *124*, 11809–11826. (c) de Visser, S. P.; Shaik, S. *J. Am. Chem. Soc.* **2003**, *125*, 7413–7424. (d) de Visser, S. P. *Chem.—Eur. J.* **2006**, *12*, 8168–8177.

(24) (a) Couture, M.; Adak, S.; Stuehr, D. J.; Rousseau, D. L. *J. Biol. Chem.* **2001**, *276*, 38280–38288. (b) Voegtle, H. L.; Sono, M.; Adak, S.; Pond, A. E.; Tomita, T.; Perera, R.; Goodin, D. B.; Ikeda-Saito, M.; Stuehr, D. J.; Dawson, J. H. *Biochemistry* **2003**, *42*, 2475–2484.
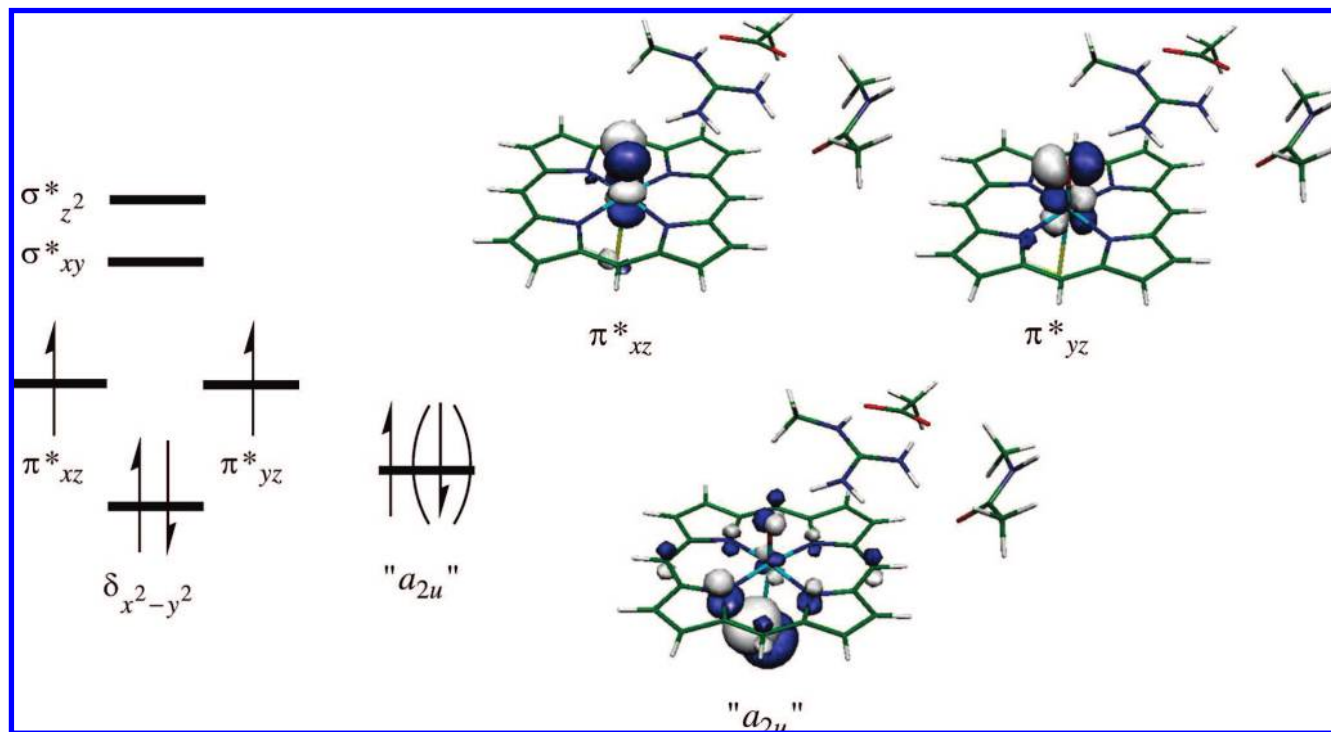
Figure 1. Orbital diagram of high-lying occupied and low-lying virtual orbitals of CpdI of NOS. Also shown are the natural orbitals of ^{4}CpdI$_A$.

therefore it is predicted that CpdI is also the active oxidant in NOS and P450 enzymes.[25] Therefore, we started our investigation of NOS enzymes on the catalytic properties of CpdI.

CpdI is a triradical system with three unpaired electrons residing in two π^* orbitals along the FeO bond (π^*_{xz}, π^*_{yz}) coupled to an unpaired heme electron (a$_{2u}$) (see Figure 1).[26] In D_{4h} symmetry the unpaired electron on the heme resides in an orbital with a$_{2u}$ symmetry and for simplicity we keep that nomenclature here. This orbital strongly mixes with a lone-pair orbital on the thiolate ligand as shown in Figure 1, but following common practice we will label this orbital as "a$_{2u}$".[14c,22,26] The high-lying occupied and low-lying virtual orbitals are dominated by the metal 3d contributions and split into 3t$_{2g}$-type and 2e$_g$-type orbitals with π^* and σ^* symmetry, respectively. As the heme is close to D_{4h} symmetry the π^* orbitals split further into a one-below-two set of orbitals. The lowest one of those ($\delta_{x^2-y^2}$) is essentially a nonbonding orbital in the xy-plane (heme-plane) and is doubly occupied in all structures discussed here. The other two π^* orbitals (π^*_{xz}, π^*_{yz}) are close to being degenerate and are singly occupied in a similar fashion as triplet oxygen. The high-lying σ^* orbitals are virtual and represent the antibonding interactions of the metal with the oxo and axial ligands ($\sigma^*_{z^2}$) and with the nitrogen atoms of the heme (σ^*_{xy}). The orbitals obtained for ^{4}CpdI$_A$ are shown on the right-hand-side of Figure 1. The shapes of the orbitals are similar for models A, B, and C for the doublet and quartet spin states as discussed here: the protonation state of arginine has little effect on the high-lying occupied and virtual orbitals of CpdI. The three singly occupied orbitals in ^{4,2}CpdI$_A$ show a close resemblance to the π^*_{xz}, π^*_{yz}, and a$_{2u}$ orbitals obtained for CpdI of P450 systems as well as with peroxidases.[22,27] Since, the spin-coupling between the two π^* orbitals and the a$_{2u}$ orbital is small, the

system appears in close-lying doublet and quartet spin states with three unpaired electrons. As shown before, this leads to two-state reactivity patterns on competing doublet and quartet spin state surfaces.[28] Therefore, TSR leads to reaction barriers on doublet as well as quartet spin state surfaces. A unique manifestation of this phenomenon appears in cases where the doublet and quartet mechanisms have different reaction mechanisms and barriers, as for instance is the case for the hydroxylation of *trans*-methyl-phenyl-cyclopropane by ^{4,2}CpdI of P450. Thus, the two spin state surfaces lead to different product distributions and product isotope effects whereby the quartet spin state mechanism leads to rearranged products while on the doublet spin state surface only unrearranged products are formed.[29] Similarly, alkene epoxidation reactions by P450 enzymes have been shown to give rise to suicidal or aldehyde byproduct that only originate from the quartet spin state surfaces owing to the lifetime of the radical intermediates.[30]

Surprisingly, the effect of the protein environment on the shapes of the orbitals is very small. Environmental perturbations from the peptide surrounding or through hydrogen-bonded ammonia molecules toward the thiolate ligand have little effect on the doublet-quartet energy gap of the systems studied. The group spin densities on the oxo-iron group are strongly polarized toward the iron atom because of the neighboring positive charge

(25) Li, H.; Poulos, T. L. *J. Inorg. Biochem.* **2005**, *99*, 293–305.

(26) Green, M. T. *J. Am. Chem. Soc.* **1999**, *121*, 7939–7940.

(27) Green, M. T. *J. Am. Chem. Soc.* **2000**, *122*, 9495–9499.

(28) (a) Shaik, S.; de Visser, S. P.; Ogliaro, F.; Schwarz, H.; Schröder, D. *Curr. Opin. Chem. Biol.* **2002**, *6*, 556–567. (b) Shaik, S.; Kumar, D.; de Visser, S. P.; Altun, A.; Thiel, W. *Chem. Rev.* **2005**, *105*, 2279–2328.

(29) (a) Kumar, D.; de Visser, S. P.; Shaik, S. *J. Am. Chem. Soc.* **2003**, *125*, 13024–13025. (b) Kumar, D.; de Visser, S. P.; Sharma, P. K.; Cohen, S.; Shaik, S. *J. Am. Chem. Soc.* **2004**, *126*, 1907–1920.

(30) (a) de Visser, S. P.; Ogliaro, F.; Harris, N.; Shaik, S. *J. Am. Chem. Soc.* **2001**, *123*, 3037–3047. (b) de Visser, S. P.; Ogliaro, F.; Shaik, S. *Angew. Chem., Int. Ed.* **2001**, *40*, 2871–2874. (c) de Visser, S. P.; Kumar, D.; Shaik, S. *J. Inorg. Biochem.* **2004**, *98*, 1183–1193. (d) Kumar, D.; de Visser, S. P.; Shaik, S. *Chem.—Eur. J.* **2005**, *11*, 2825–2835.
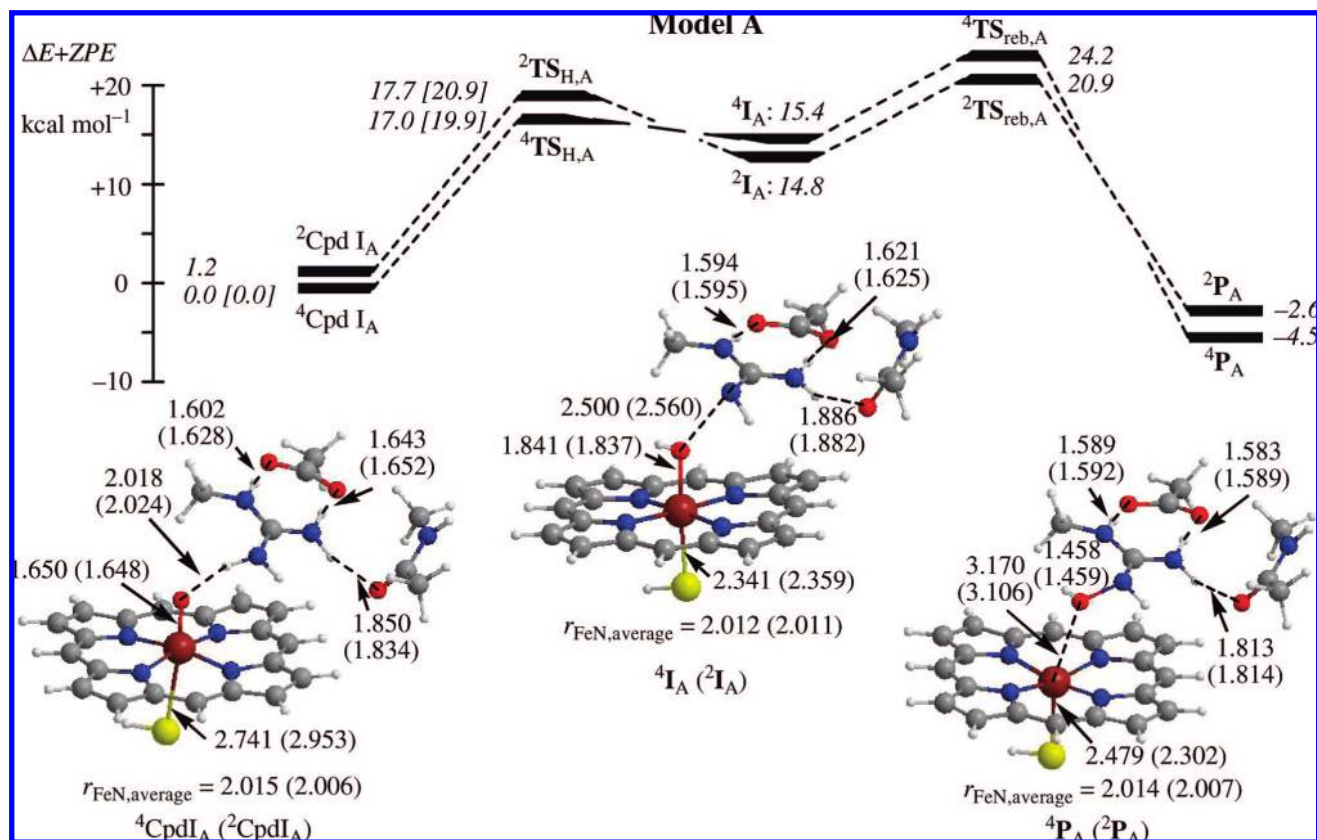
Figure 2. Potential energy profile of the hydroxylation of L-arginine by $^{4,2}CpdI_A$. All energies are in kcal mol^{-1} relative to $^4CpdI_A$. Also shown are optimized geometries of reactant, intermediate, and product complexes with bond lengths in angstroms. In square brackets are given the energies (using basis set B2 and ZPE corrections with basis set B1) of the system with two additional hydrogen-bonded ammonia molecules.

of the arginine. As before, in the gas phase a large group spin density on the thiolate is observed, but two hydrogen-bonded ammonia molecules lower the thiolate spin density to 0.48 while the one on the heme increases it to 0.47. These values are in line with group spin densities observed with quantum mechanical/molecular mechanics (QM/MM) on CpdI of P450 and NOS.[17,31] Below we will discuss the electronic properties in an enzyme-mimicked environment in more detail.

Catalytic Properties of Model A. Subsequently, we investigated the hydrogen abstraction reaction of protonated L-arginine by $^{4,2}CpdI_A$ and the results are shown in Figure 2. The reaction is stepwise starting from $^{4,2}CpdI_A$ with a hydrogen abstraction from the substrate via barrier $TS_{H,A}$ leading to a hydroxo-iron complex (I_A). A subsequent radical rebound process via barrier $TS_{reb,A}$ leads to N^ω-hydroxo-arginine products (P_A).

As shown in the previous section, the ground-state of CpdI has a close lying doublet and quartet spin states which result in two-state reactivity patterns. The reaction starting from $^{4,2}CpdI_A$ has a relatively large hydrogen abstraction barrier of 17.0 (17.7) kcal mol^{-1} via $^4TS_{H,A}$ ($^2TS_{H,A}$). In the transition states an electron is transferred from the substrate into the a_{2u} molecular orbital leading to a radical intermediate species. A subsequent large rebound barrier on both the low-spin and high-spin surfaces leads to products in an overall slightly exothermic reaction. The exothermicity of reaction is much lower as was obtained for

alkane hydroxylation by P450 models and QM/MM, where typically values of around 30 kcal mol^{-1} or larger were found.[31,32]

Geometrically, the optimized geometries along the reaction mechanism show similarities with structures obtained for alkane hydroxylation by P450 models. Optimized geometries of $^{4,2}CpdI_A$, $^{4,2}I_A$ and $^{4,2}P_A$ are shown at the bottom of Figure 2. The oxo-iron distances are short: 1.650 and 1.648 Å for $^4CpdI_A$ and $^2CpdI_A$, respectively. This is a typical bond length and has been observed before for CpdI systems of P450, peroxidases, and catalases.[22,26,33] The Fe–S distances, by contrast, are relatively long here, that is, 2.741 and 2.953 Å for $^4CpdI_A$ and $^2CpdI_A$, and significantly longer than the same distance in P450 CpdI obtained with either DFT models or QM/MM. Attempts to shorten the Fe–S distance and reoptimizing the geometry led to the same structure as depicted in Figure 2. An Fe–S distance of longer than 2.7 Å was also observed for a ^4CpdI model calculation on P450 with cysteinate axial ligand rather than the thiolate used here.[31] Therefore, despite $^4CpdI_A$ having a relative long Fe–S distance these types of bond lengths have been observed before and reflect the weak interaction of two second row elements. The Fe–S distance in the intermediate and product complexes is much shorter than in $^{4,2}CpdI_A$ and closer to typical values of around 2.4 Å for iron–sulfur distances.[23] The bond distances calculated here for the inter-

(31) Schöneboom, J. C.; Lin, H.; Reuter, N.; Thiel, W.; Cohen, S.; Ogliaro, F.; Shaik, S. *J. Am. Chem. Soc.* **2002**, *124*, 8142–8151.

(32) (a) de Visser, S. P.; Kumar, D.; Cohen, S.; Shacham, R.; Shaik, S. *J. Am. Chem. Soc.* **2004**, *126*, 8362–8363. (b) Altun, A.; Shaik, S.; Thiel, W. *J. Am. Chem. Soc.* **2007**, *129*, 8978–8987.

(33) Bathelt, C. M.; Zurek, J.; Mulholland, A. J.; Harvey, J. N. *J. Am. Chem. Soc.* **2005**, *127*, 12900–12908.
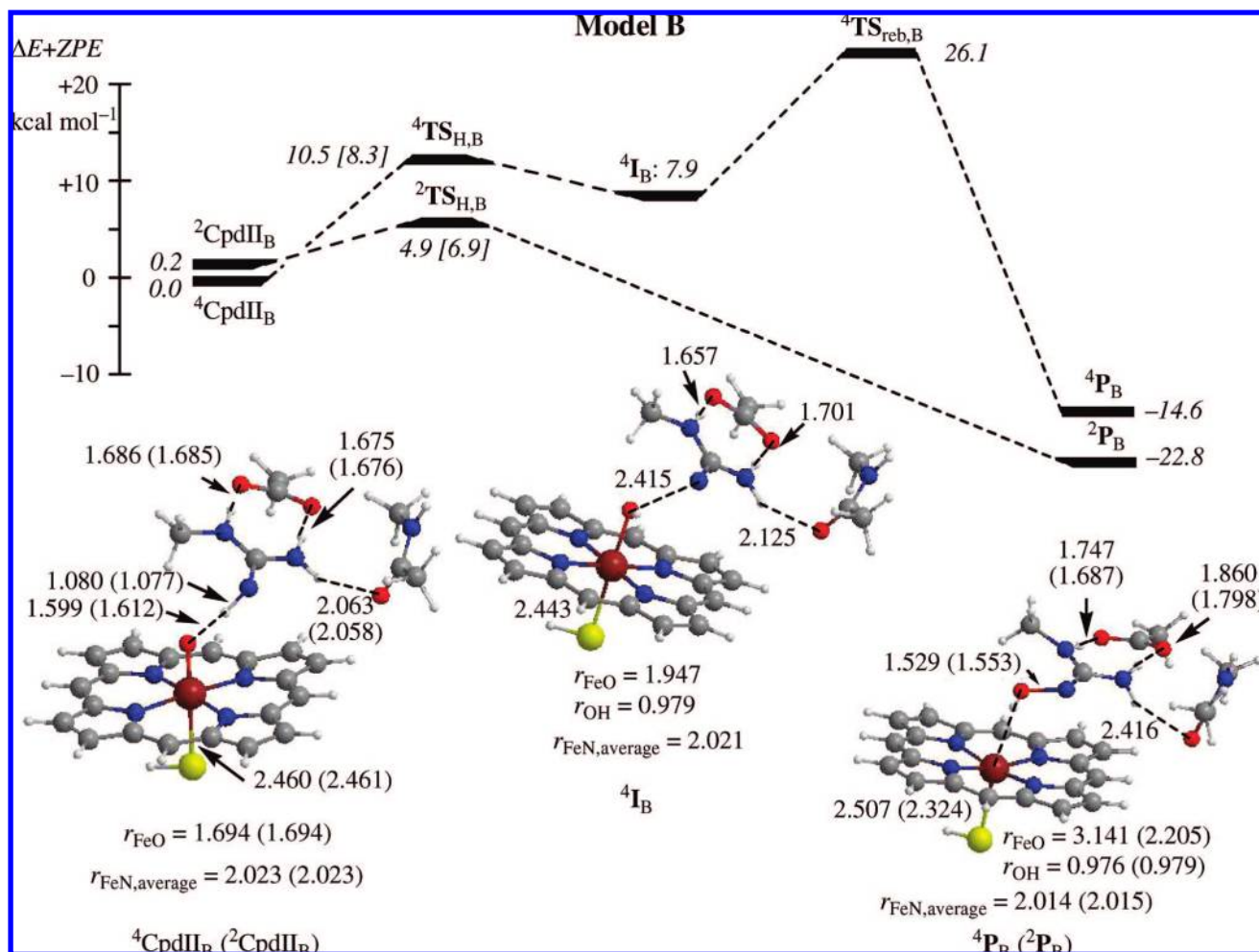
Figure 3. Potential energy profile of the hydroxylation of L-arginine by ^{4,2}CpdII$_B$. All energies are in kcal mol^{-1} relative to ^{4}CpdII$_B$. Also shown are optimized geometries of reactant, intermediate, and product complexes with bond lengths in angstroms. In square parenthesis are given the energies (using basis set B2 and ZPE corrections with basis set B1) of the system with two additional hydrogen-bonded ammonia molecules.

mediate and product complexes compare well with those obtained for the hydroxylation of alkanes by P450 models.[32a] Only minor differences in the hydrogen-bond lengths between the various amino acids are observed in ^{4,2}CpdI$_A$, ^{4,2}I$_A$, and ^{4,2}P$_A$.

The addition of two hydrogen-bonded ammonia molecules mimicking the interactions of Trp$_{180}$ with the thiolate ligand raises the hydrogen abstraction barriers by only a few kcal mol^{-1}. Moreover, no significant electronic differences are observed in this reaction step and the reaction mechanism remains the same. The group spin densities in the transition states stay virtually unchanged with respect to the models without extra hydrogen-bonding ammonia molecules toward the thiolate ligand. It appears, therefore, that the DFT model is a faithful mimic of the enzyme active site region and correctly predicts the mechanism and energetics.

Consequently, the small reaction exothermicity and high hydrogen abstraction and rebound barriers as obtained here for protonated L-arginine hydroxylation by ^{4,2}CpdI$_A$ imply that this is an unlikely process in the enzyme. By contrast, ^{4,2}CpdI of P450 and peroxidases are known to catalyze hydrogen abstraction reactions with small barriers, as shown over and over again with DFT models and QM/MM.[31,34] We decided to investigate whether an initial deprotonation of the substrate affects the reaction barriers and exothermicities.

Catalytic Properties of Model B. Subsequently, we removed a proton from position H$_b$ (see Scheme 3 above) to create model B: the deprotonated reactant ^{4,2}CpdI$_B$. The hydroxylation mechanism of L-arginine by ^{4,2}CpdI$_B$ as well as optimized geometries of the local minima is shown in Figure 3. Although, formally ^{4,2}CpdI$_B$ is an oxo-iron species with a nearby neutral arginine molecule, during the geometry optimization a one-electron transfer occurred and it is in fact the one electron reduced form of CpdI called compound II (CpdII) with a nearby arginine cation radical: ^{4,2}CpdII$_B$ = ^{3}CpdII·^{2}Arg$^{+•}$. Attempts to swap molecular orbitals to create a ^{4,2}CpdI·^{1}Arg couple failed and converged back to the ^{3}CpdII·^{2}Arg$^{+•}$ situation. Therefore, the electron transfer from neutral arginine to CpdI is energetically favorable (at least in the gas-phase) and will produce CpdII quickly.

Figure 3 shows the potential energy profile of arginine cation radical hydroxylation by ^{4,2}CpdII$_B$ of NOS (model B). The hydrogen abstraction reaction of this model is feasible with significantly lower barriers than the ones obtained for ^{4,2}CpdI$_A$. In principle, the reaction mechanism on the quartet spin state

(34) (a) Kamachi, T.; Yoshizawa, K. *J. Am. Chem. Soc.* **2003**, *125*, 4652–4661. (b) Bathelt, C. M.; Ridder, L.; Mulholland, A. J.; Harvey, J. N. *Org. Biomol. Chem.* **2004**, *2*, 2998–3005. (c) Kumar, D.; de Visser, S. P.; Sharma, P. K.; Derat, E.; Shaik, S. *J. Biol. Inorg. Chem.* **2005**, *10*, 181–189.

surface is similar to that found for model A but there are some critical differences. On the high-spin surface a small hydrogen abstraction barrier of 10.5 kcal mol^{-1} leads to a stable hydroxo-iron complex, but a very high rebound barrier needs to be crossed to reach products. The overall barrier for the reaction on the high-spin surfaces is 26.1 kcal mol^{-1}, which implies that the system will be a sluggish oxidant and unlikely to play a key role in the reaction mechanism. On the low-spin surface, by contrast, a totally different picture emerges. The reaction mechanism starting from ^{2}CpdII$_B$ leads via a tiny and concerted hydrogen abstraction barrier of 4.9 kcal mol^{-1} directly to products in a reasonable exothermic process. This implies that CpdII is a powerful catalyst and able to hydroxylate arginine cation radical efficiently. In earlier work, we showed that the hydroxylation of alkanes by P450 models usually encounters a significant rebound barrier on the high-spin surface, whereas the low-spin surface either has a negligible rebound barrier after a stable hydroxo-iron complex or is concerted and leading to products immediately.[35] The NOS CpdII model B follows a P450-type reaction mechanism with competing high-spin and low-spin surfaces of which the high-spin is stepwise with significant rebound barrier, whereas the low-spin is concerted. The big difference with the P450 mechanisms from the literature is the fact that CpdII is a possible catalyst of hydroxylation reactions here, while all P450 studies seemed to have ruled out CpdII as an alternative catalyst.[32b] Below we will discuss these differences further and explain why CpdII can act as a catalyst of hydroxylation reactions here.

Additional hydrogen-bonding interactions through ammonia molecules that mimic the interactions in the protein environment have a small effect on the reaction barriers. Thus, ^{2}TS$_{H,B}$ is raised to 6.9 kcal mol^{-1}, while ^{4}TS$_{H,B}$ drops to 8.3 kcal mol^{-1}. Nevertheless, the barrier via ^{2}TS$_{H,B}$ remains the rate determining step in the reaction mechanism with an overall barrier well below that of ^{4}TS$_{H,A}$ in the previous section. Moreover, the high-spin mechanism will be a slow process in any case owing to the high rebound barrier ^{4}TS$_{reb,B}$ that is rate determining. Therefore, the protein environment has little effect on the calculated reaction mechanisms and the gas-phase results are reliable and reproduced in an enzyme mimicked model.

Because arginine is deprotonated in ^{4,2}CpdII$_B$ the hydrogen-bonding interactions of the substrate with Glu$_{363}$ and Trp$_{358}$ also have weakened, and these distances are significantly longer in ^{4,2}CpdII$_B$ then in ^{4,2}CpdI$_A$ above. Especially, the hydrogen-bond length between H$_c$ of arginine cation radical with the carbonyl oxygen atom of the peptide bond is enhanced to 2.063 (2.058) Å for ^{4}CpdII$_B$ (^{2}CpdII$_B$).

In summary, deprotonation of arginine transfers an electron to ^{4,2}CpdI$_B$ to form ^{3}CpdII and an arginine cation radical. A subsequent low-barrier hydrogen abstraction mechanism on the low-spin surface leads to N^ω-hydroxo-arginine with an exo-thermicity of more than 20 kcal mol^{-1}. However, the alternative quartet spin reactant is a sluggish oxidant with much higher barriers, so that NOS will react via single-state reactivity on a dominant doublet spin state surface. DFT calculations on hydroxylation and sulfoxidation reactions catalyzed by P450

enzyme models showed that although CpdI has close-lying quartet and doublet spin states, often only one of the two is active.[23c,36]

Catalytic Properties of Model C. For completeness we also calculated a system with a deprotonated arginine whereby the proton is removed from the H$_d$ position in Scheme 3. The hydroxylation mechanism of ^{4,2}CpdII$_C$ and optimized geometries of the critical points are shown in Figure 4. Geometrically, most structures are very similar to the ones obtained for model B. Similarly to model B also here the reactant has ^{3}CpdII·^{2}Arg$^{+\bullet}$ configuration rather than ^{4}CpdI·^{1}Arg. The difference between model B and model C is that one hydrogen bond between the substrate and Glu$_{363}$ is missing in model C, which makes ^{4}CpdII$_C$ 11.5 kcal mol^{-1} less stable than ^{4}CpdII$_B$. Also, as a result of this missing hydrogen bond, the radical intermediate is destabilized and as a consequence the reaction barriers are higher than those observed for model B, but not as high as the ones for model A. In model C, the hydrogen abstraction barrier is only a few tenths of a kcal mol^{-1} higher in energy than the radical intermediate. On the low-spin surface a negligible rebound barrier leads to hydroxylation products, but on the high-spin surface a high rebound barrier of 16.2 kcal mol^{-1} is encountered. This implies that similarly to model B only the low-spin surface will be reactive toward substrates. The exo-thermicity leading to products is similar to the one observed in model B, but there are some big geometric differences. First of all, the hydrogen bond between the carbonyl group of the Trp$_{358}$ peptide bond is broken and instead the amide hydrogen atom forms a hydrogen bond with the amine group of the substrate. It is unlikely that this rotation is possible in the enzyme, but it clearly shows that the hydrogen bond between the carbonyl oxygen and substrate is weakened in this model. Moreover, in addition the carboxylic acid group of Glu$_{363}$ rotates as it can only form one hydrogen bond with the substrate. Therefore, in models A and B the substrate will be held in a much tighter configuration than in model C and the system is also more stabilized because of more hydrogen-bonding interactions. Thus, the hydrogen-bonding interactions, the higher reaction barriers, and the movement of the surrounding peptide seem to rule out model C as a possible mechanism of arginine hydroxylation by NOS enzymes.

Environmental Perturbations on the Reaction Mechanisms. Extensive theoretical studies of heme systems with a cysteinate axial ligand showed that the electronic properties of CpdI are determined by the local environment of the thiolate ligand.[17,22,31] Thus, in the enzyme the thiolate group of the axial cysteinate ligand of the heme accepts hydrogen bonds from nearby peptide groups, for example, Trp$_{180}$ in the 4NSE pdb file, see Scheme 2 above. In the past we mimicked these interactions through the addition of two hydrogen-bonded ammonia molecules to the system.[22a] Here we used the same procedure and indeed the relative energies of the barriers are reproduced as shown above in Figures 3 and 4. To further establish that ^{4}CpdI$_A$ and ^{4}CpdII$_B$ are correctly described by our model we did full geometry optimizations of ^{4}CpdI$_A$·2NH$_3$ and ^{4}CpdII$_B$·2NH$_3$ and the results are shown in Figure 5. As follows from Figure 5, a full geometry optimization with two extra hydrogen-bonded ammonia molecules that mimic the interactions in the protein environment retains the essential features of the structure and only minor differences in bond lengths are obtained. As a matter

(35) Shaik, S.; Cohen, S.; de Visser, S. P.; Sharma, P. K.; Kumar, D.; Kozuch, S.; Ogliaro, F.; Danovich, D. *Eur. J. Inorg. Chem.* **2004**, 207–226.

(36) Sharma, P. K.; de Visser, S. P.; Shaik, S. *J. Am. Chem. Soc.* **2003**, *125*, 8698–8699.
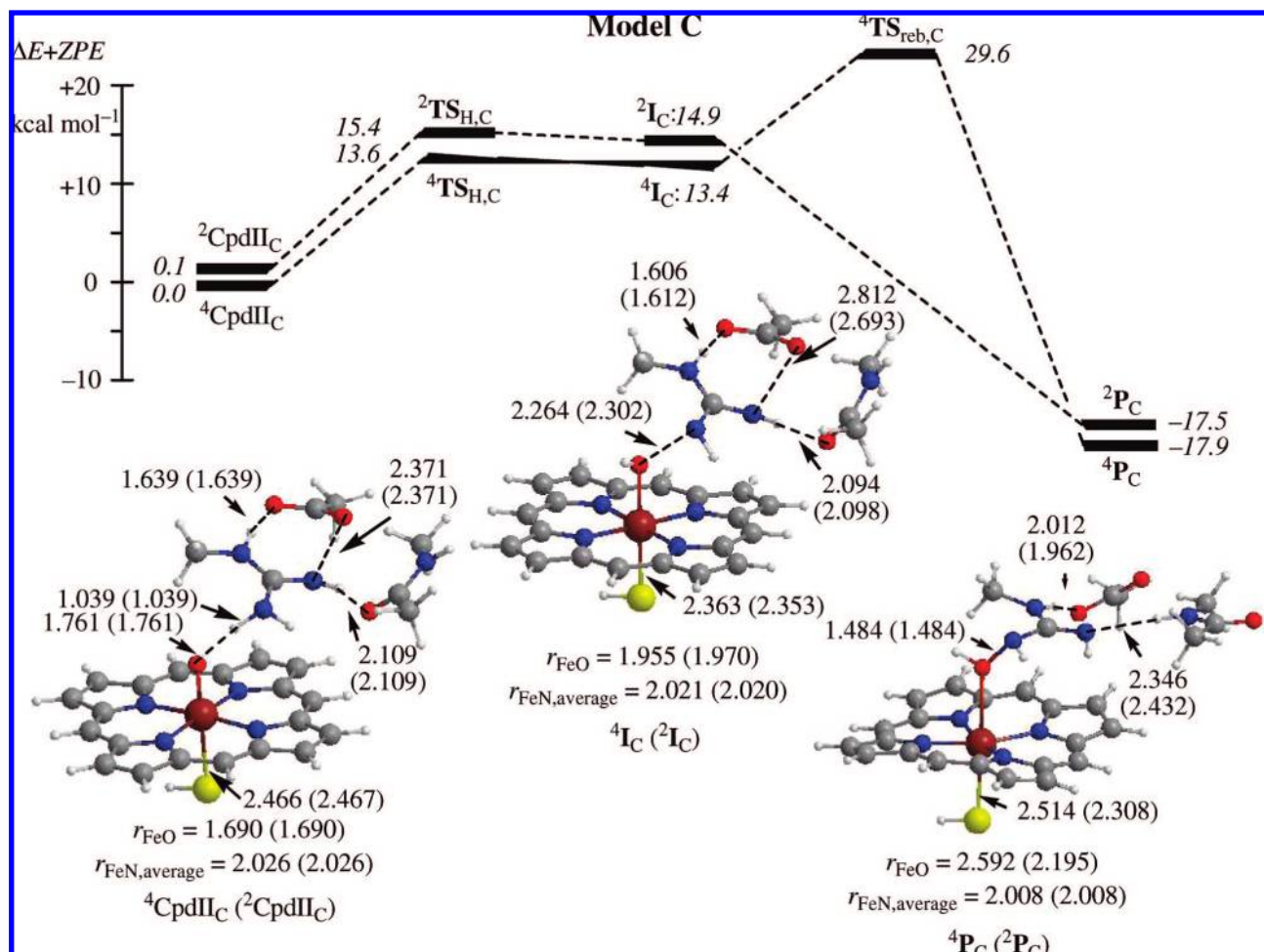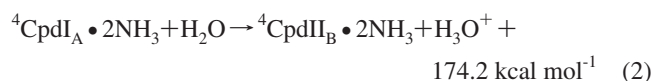
Figure 4. Potential energy profile of the hydroxylation of L-arginine by ^{4,2}CpdII$_C$. All energies are in kcal mol^{-1} relative to ^{4}CpdII$_C$. Also shown are optimized geometries of reactant, intermediate, and product complexes with bond lengths in angstroms.

of fact most distances are with 0.005 Å between the systems with and without hydrogen-bonded ammonia molecules. The only distances that change slightly with hydrogen-bonding interactions are the substrate-oxo distances and in the case of ^{4}CpdII$_B$, also the Fe–S distance.

Also shown in Figure 5 are the group spin densities of the systems with and without hydrogen-bonded ammonia molecules. In the case of ^{4}CpdII$_B$·2NH$_3$ most group spin densities are similar to those obtained for ^{4}CpdII$_B$. Therefore, the deprotonated system has the same electronic configuration regardless of whether hydrogen bonding toward the thiolate is included or not. This is not surprising since the thiolate has little radical character and nearby positive charges from the protons of the donating hydrogen-bonding groups will cause little disruption of the electronic configuration. By contrast, in ^{4}CpdI$_A$ the thiolate ligand has partial radical character owing to the mixing of the a_{2u} heme orbital with a π_S sulfur orbital. As a consequence, the thiolate ligand has spin density of 0.63 in ^{4}CpdI$_A$ the gas-phase. However, hydrogen-bonding interactions toward thiolate change the charge distribution around the thiolate and pushes electron density from the thiolate to the heme, and the spin density drops to $\rho_{SH} = 0.41$. These spin density changes are similar to those observed before for P450 gas-phase models versus QM/MM.[22a,31] Despite these large differences in electronic situation between ^{4}CpdI$_A$ and ^{4}CpdI$_A$·2NH$_3$ the reaction barriers of the hydroxylation processes stay virtually the same: the hydrogen abstraction barrier ^{4}TS$_{H,A}$·2NH$_3$ is 19.9 kcal mol^{-1}

higher in energy than ^{4}CpdI$_A$·2NH$_3$. Therefore, ^{4,2}CpdI$_A$ is a sluggish oxidant that is unable to hydroxylate protonated arginine. The hydroxylation reaction starting from ^{4}CpdII$_B$· 2NH$_3$ encounters a hydrogen abstraction barrier of 6.9 kcal mol^{-1} via ^{2}TS$_{H,A}$·2NH$_3$, which implies that ^{4,2}CpdII$_B$ is an efficient catalyst of hydroxylation reactions. Thus, the gas-phase models are faithful mimics of the enzyme active site of NOS and predict reaction mechanisms and barriers correctly.

As a comparison we calculated the proton transfer energies from ^{4}CpdI$_A$ and ^{4}CpdI$_A$·2NH$_3$ to water leading to ^{4}CpdII$_B$ and ^{4}CpdII$_B$·2NH$_3$ and H$_3$O$^+$, eq 1 and eq 2. These two reactions have endothermicities of 173.2 and 174.2 kcal mol^{-1}, that is, are within 1 kcal mol^{-1}. Clearly, environmental effects such as hydrogen-bonding ammonia molecules toward the thiolate group hardly influence the basicity of the arginine and the electron affinity of CpdI. Therefore, these type of reaction energies can give useful predictions regarding proton and electron transfer processes as will be shown later.

$$^4CpdI_A + H_2O \rightarrow {}^4CpdII_B + H_3O^+ + 173.2 \text{ kcal mol}^{-1} \quad (1)$$

$$^4CpdI_A \cdot 2NH_3 + H_2O \rightarrow {}^4CpdII_B \cdot 2NH_3 + H_3O^+ + 174.2 \text{ kcal mol}^{-1} \quad (2)$$

Discussion

In this work we present DFT studies on the first step in the reaction mechanism catalyzed by NOS enzymes, namely the

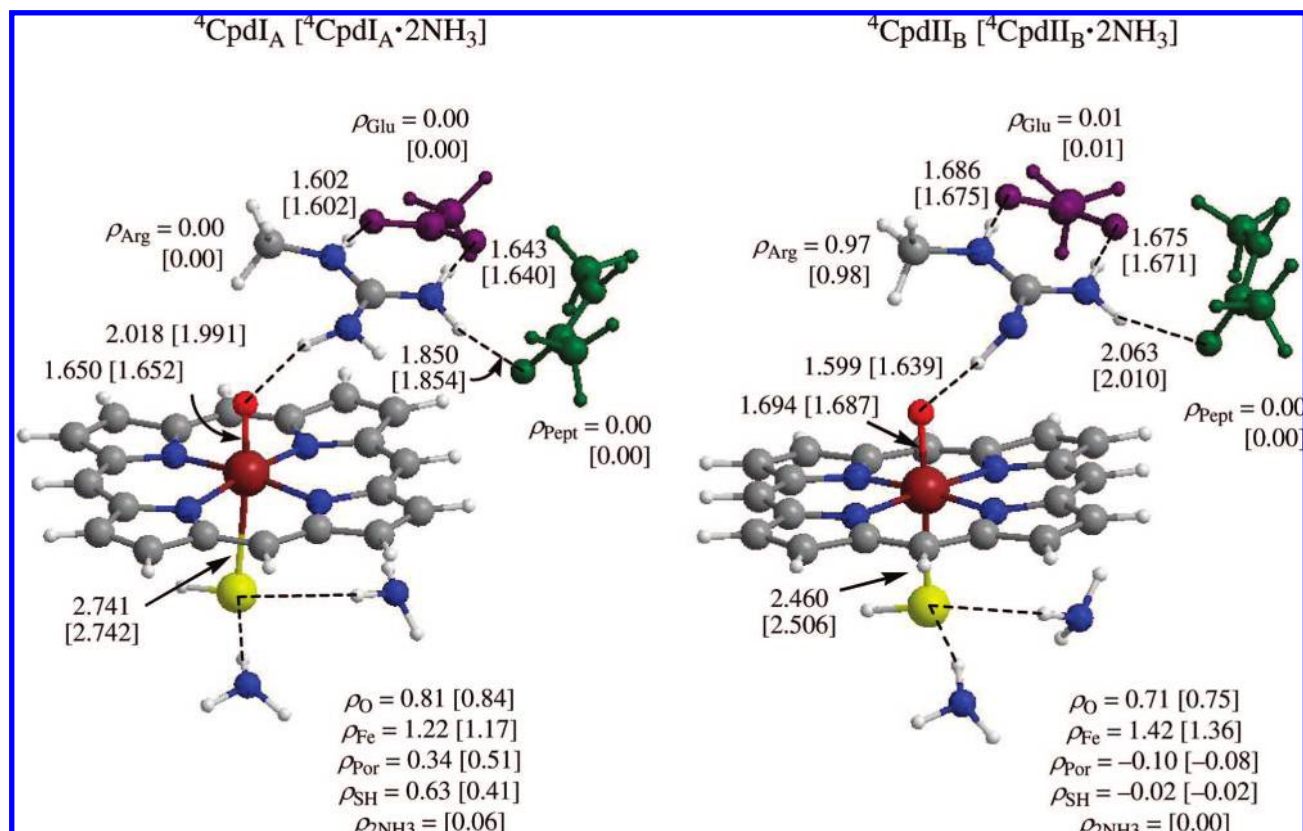**Figure 5.** Optimized geometries of $^4CpdI_A$ [$^4CpdI_A \cdot 2NH_3$] (left-hand-side) and $^4CpdII_B$ [$^4CpdII_B \cdot 2NH_3$] (right-hand-side). Bond lengths (in angstroms) and group spin densities (ρ) are given.

hydroxylation of L-arginine by the oxo-iron species in the catalytic cycle. Thus, in order to find out in what protonation state the substrate is bound, we studied the hydroxylation of protonated arginine and neutral arginine by the oxo-iron active species using models **A**, **B**, and **C**. The model with protonated arginine as substrate (model **A**) has the highest hydrogen abstraction barriers: 17.0 and 17.7 kcal mol^{-1} in the quartet and doublet spin states, respectively. In addition, a substantial rebound barrier makes the overall barrier of the reaction well above 20 kcal mol^{-1} on both spin-state surfaces. Moreover, the overall reaction for model **A** is close to thermoneutral, whereas the ones for model **B** and **C** are about 20 kcal mol^{-1} exothermic. Therefore, on the basis of these energies it is unlikely that a protonated substrate is being hydroxylated during the catalytic cycle of NOS enzymes. However, because the pK_a of the methylguanidinium group of arginine is approximately 12 at room temperature it is likely that arginine binds in the protonated form, so that the substrate must be deprotonated somewhere in the catalytic cycle prior to the hydroxylation step. In the following we will discuss proton and hydrogen atom transfer reactions and establish what the most likely scenario for deprotonation of arginine in the catalytic cycle of NOS is and its subsequent hydroxylation.

Thermodynamics of Hydrogen and Proton Transfer from ArgH$^+$. To gain insight into possible protonation states of the substrate and how exo- or endothermic the various possible hydrogen or proton transfer processes are, we ran a series of extra calculations on isolated substrate in its various protonation states, see Figure 6. The strength of the R-H bond in molecule RH is calculated from the bond dissociation energy (BDE$_{RH}$)

as defined in eq 3. Here we will focus on BDE$_{NH}$, where an N−H bond is broken from either a protonated or neutral arginine.

$$R\text{-}H \rightarrow R\bullet + H\bullet + BDE_{RH} \qquad (3)$$

The basicity of the substrate or enthalpy of proton transfer (ΔH_{PT}) is determined from the ability of the substrate to donate a proton to a water molecule, eq 4, because it has been anticipated that at least one proton in the catalytic cycle is relayed through a chain of water molecules from the solvent to the active site.[3,13,17,37]

$$R-H + H_2O \rightarrow R^- + H_3O^+ + \Delta H_{PT} \qquad (4)$$
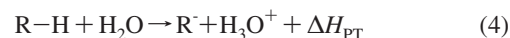
Values of BDE$_{NH}$ and ΔH_{PT} were determined from single point UB3LYP/B2 calculations on fully optimized geometries at the UB3LYP/B1 level of theory and are reported at ΔE + ZPE level of theory as above with ZPE corrections obtained with basis set B1. Previous work of ours showed that DFT at this level of theory can reproduce experimental hydrogen abstraction enthalpies accurately.[32a]

Figure 6 shows the reaction energies for proton or hydrogen atom transfer from protonated methylguanidinium (ArgH$^+$) and the associated energies. Arg$_b$ and Arg$_d$ are the neutral substrates used in models **B** and **C** above, whereby the atoms are labeled as in Scheme 3 above. As follows from Figure 6 deprotonation of the H$_a$, H$_b$, and H$_d$ positions of ArgH$^+$ is endothermic by about 76 kcal mol^{-1} and all positions are equally strong. An endothermic reaction is expected since arginine is a stronger

(37) Crane, B. R.; Arvai, A. S.; Ghosh, D. K.; Wu, C.; Getzoff, E. D.; Stuehr, D. J.; Tainer, J. A. *Science* **1998**, *279*, 2121–2126.
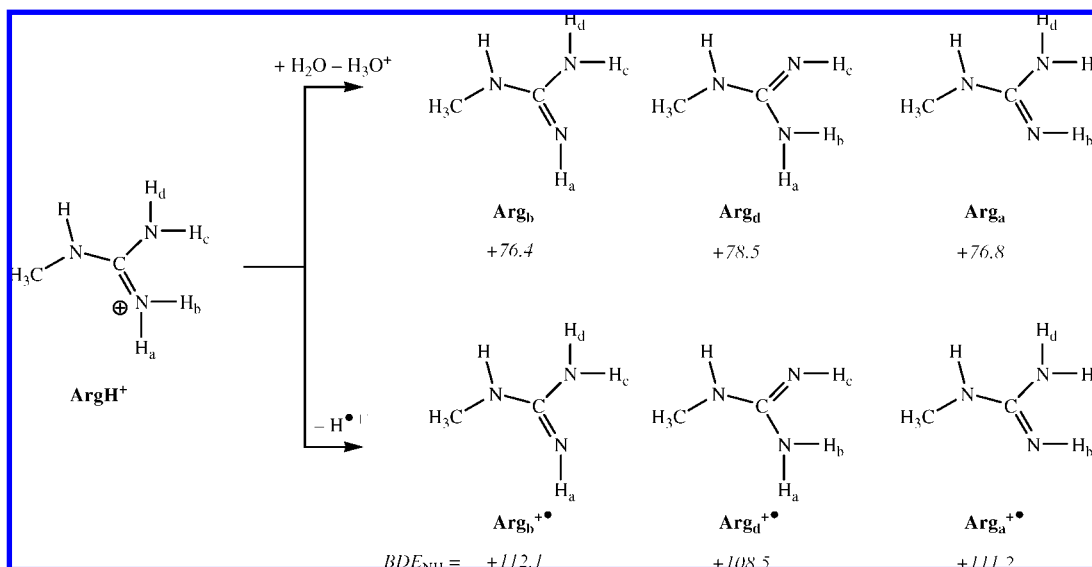
Figure 6. Relative energies of deprotonation (top) and hydrogen abstraction (bottom) from protonated methylguanidinium ($ArgH^+$). The subscript gives the label of the hydrogen atom/proton that is removed in the process. All data are in kcal mol^{-1} and include ZPE corrections. The deprotonation reaction is calculated relative to water and H_3O^+ as a reference.

base than water. Thus, in principle deprotonation of protonated arginine can take place on any of the positions with almost equal energetic costs. Also shown in Figure 6 are the hydrogen abstraction energies from $ArgH^+$: BDE$_{NH}$. These bond dissociation energies are very high (in the order of 110 kcal mol^{-1}) and are of comparable value to the C—H bond strength in methane.[32a] Since, oxo-iron species are not known to catalyze methane hydroxylation it is unlikely that a hydrogen abstraction from $ArgH^+$ takes place. A proton abstraction is much less endothermic but will depend on the ability of CpdI to abstract a proton, which we will discuss below. Therefore, unless CpdI can take up a proton from $ArgH^+$, the deprotonation of $ArgH^+$ will take place at an earlier step in the catalytic cycle.

Thermodynamics of Hydrogen and Proton Transfer from Neutral Arginine (Arg^0). Subsequently, we calculated the proton and hydrogen atom transfer energies from deprotonated arginine at the H_b position (Arg$_b$) and the results are shown in Figure 7. For completeness we also calculated the energies starting from Arg$_d$ (see Supporting Information), but the energies are virtually the same as the ones shown here for Arg$_b$. Nevertheless, it is unlikely that $ArgH^+$ is deprotonated at the H_d position in the enzyme as it is locked in strong hydrogen-bonding interactions with Glu$_{363}$, which is too weak a base to accept a proton from $ArgH^+$. Deprotonation of a neutral arginine by water is highly endothermic by 220 kcal mol^{-1}, Figure 7.

The hydrogen abstraction energy of Arg$_b$ and Arg$_d$ is substantially lowered in comparison to that of protonated arginine by about 17 kcal mol^{-1}, which means that the N—H bond in neutral arginine is much weaker and as a result is easier to hydroxylate than the one in protonated arginine. Based on the BDE$_{NH}$ values it can be concluded that neutral arginine is the most likely substrate in the hydroxylation step of NOS enzymes. Indeed, the reaction barriers obtained for model B and C are significantly lower than those observed for model A in agreement with the weaker N—H bond strength of Arg$_b{}^0$ and Arg$_d{}^0$ as opposed to the one in $ArgH^+$. As will be shown in the next section the N—H bond strength of Arg$_b{}^0$ and Arg$_b{}^{+•}$ are very close in energy so that CpdI and CpdII are not expected to show reactivity differences. In particular, the barrier via ^2TS_B is very low (4.9 kcal mol^{-1}) and is not succeeded by a larger
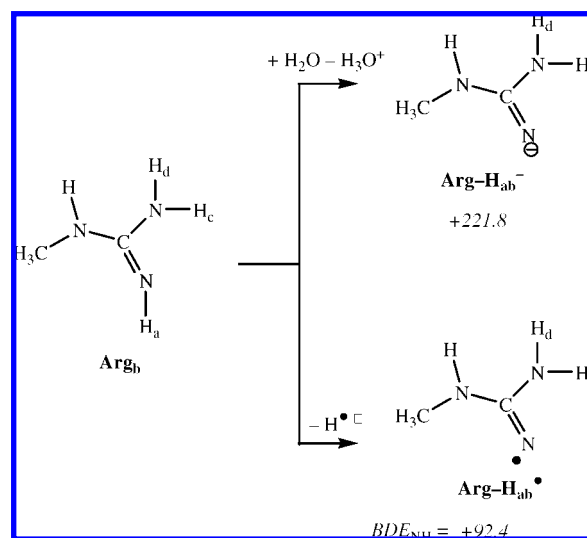

Figure 7. Relative energies of deprotonation (top) and hydrogen abstraction (bottom) from a neutral arginine molecule (Arg$_b$). All data are in kcal mol^{-1} and include ZPE corrections. The deprotonation reaction is calculated relative to water and H_3O^+ as a reference.

rebound barrier. Moreover, the exothermicity of the overall reaction is enhanced in model B with respect to model A due to the difference in strength of the N—H bond in the substrate.

How Does the Substrate Fit into the Catalytic Cycle and What Is Its Protonation State? To find out whether the substrate can actively take part in the catalytic cycle of NOS enzymes by donating a proton, we calculated the proton affinities of some of the key species in the catalytic cycle after dioxygen binding but without the protein surrounding, see Figure 8. Note, that the enthalpy of proton transfer in Figure 8 has been calculated relative to Arg$_b{}^0$ and $ArgH^+$ as a reference point. The models chosen were iron protoporphyrin IX (without side chains) with thiolate as axial ligand and variable distal ligand. Although most of these structures have been calculated before, we reoptimized each intermediate with the same procedures as elsewhere in this work so that the energies can be used to calculate reaction energies. Generally, the optimized geometries and relative
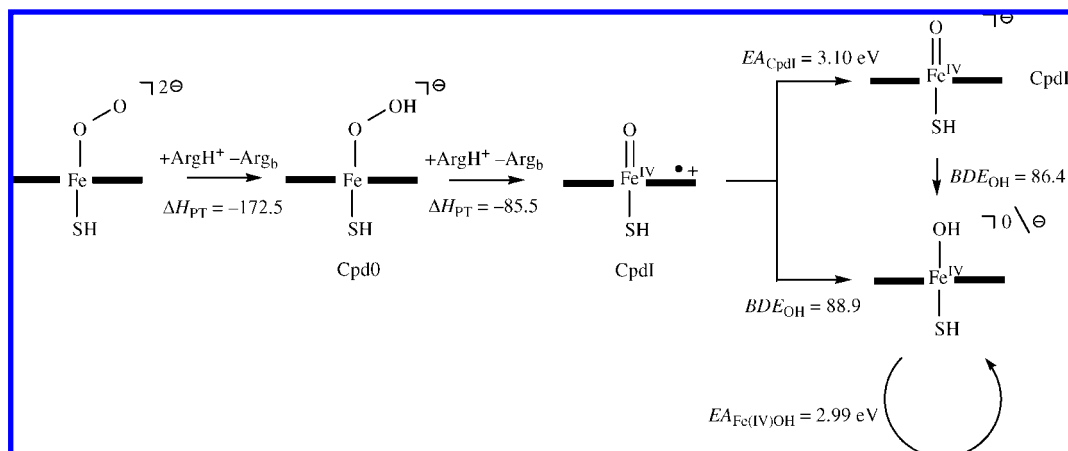
Figure 8. Relative energies of proton transfer and electron transfer mechanisms of possible catalytic cycle intermediates. The deprotonation reaction is calculated relative to $ArgH^+$ and Arg_b as a reference and is in kcal mol^{-1}.

Scheme 4. The Catalytic Cycle of NOS Enzymes Starting from the Reduced Dioxygen-Bound Complex as Derived from DFT Calculations Reported in This Work
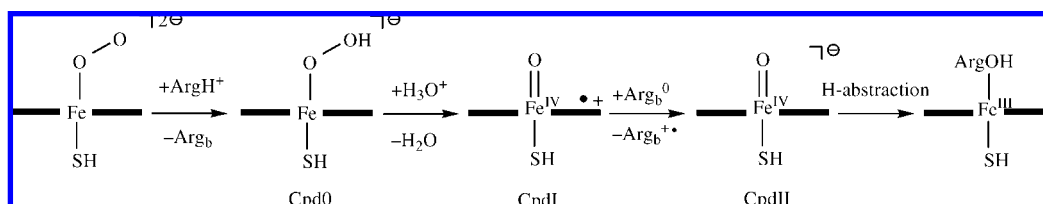
energies obtained for the catalytic cycle intermediates are in good agreement with those from the literature.[26,28,31,33,38]

The catalytic cycle starts with substrate binding followed by a reduction of the heme, dioxygen binding, and a second reduction of the heme to create the FeOO^{2-} species.[28,39] This intermediate is protonated to form the hydroperoxo—iron complex (compound 0, Cpd0) that in its turn is protonated to form the oxo-iron active species. We calculated the gas-phase proton affinities with respect to Arg^0 and ArgH$^+$ for these two steps in the catalytic cycle, see Figure 7. Both protonation steps are highly exothermic by 172.5 and 85.5 kcal mol^{-1}, respectively, which implies that both the FeOO^{2-} and Cpd0 can easily pick up a proton from a ArgH$^+$ and even easier from H$_3$O$^+$.

The hydrogen abstraction reaction of protonated arginine by CpdI to give a hydroxo-iron (FeOH) and a cation radical arginine (eq 5) is calculated to be endothermic by 22.3 kcal mol^{-1} for isolated reactants. Indeed formation of a hydroxo-iron complex in Figure 2 above was found to be endothermic by 15 kcal mol^{-1}, which implies that hydrogen-bonding interactions due to the protein environment in model A stabilize the hydroxo-iron complex by about 8 kcal mol^{-1} but the reaction is still highly endothermic. Consequently, it is unlikely that protonated arginine is the substrate that is hydroxylated by CpdI.
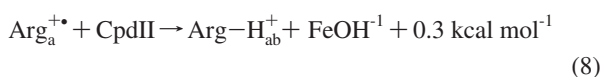
$$ArgH^+ + CpdI \rightarrow Arg_a^{+\bullet} + FeOH^0 + 22.3 \text{ kcal mol}^{-1} \quad (5)$$

(38) (a) Rydberg, P.; Sigfridsson, E.; Ryde, U. *J. Biol. Inorg. Chem.* **2004**, *9*, 203–223. (b) Groenhof, A. R.; Swart, M.; Ehlers, A. W.; Lammertsma, K. *J. Phys. Chem. A* **2005**, *109*, 3411–3417. (c) Schöneboom, J. C.; Neese, F.; Thiel, W. *J. Am. Chem. Soc.* **2005**, *127*, 5840–5853. (d) Groenhof, A. R.; Ehlers, A. W.; Lammertsma, K. *J. Am. Chem. Soc.* **2007**, *129*, 6204–6209.
(39) Zhu, Y.; Nikolic, D.; Van Breemen, R. B.; Silverman, R. B. *J. Am. Chem. Soc.* **2005**, *127*, 858–868.
(40) (a) Ogliaro, F.; de Visser, S. P.; Cohen, S.; Sharma, P. K.; Shaik, S. *J. Am. Chem. Soc.* **2001**, *124*, 2806–2817. (b) Park, M. J.; Lee, J.; Suh, Y.; Kim, J.; Nam, W. *J. Am. Chem. Soc.* **2006**, *128*, 2630–2634.

Figure 6 above predicted an energetically favorable proton transfer over hydrogen atom transfer from ArgH$^+$ therefore we calculated the alternative proton transfer reaction (Equation 6) to give a cationic hydroxo-iron moiety and neutral arginine. However, as follows this reaction is endothermic by 85.9 kcal mol^{-1} which implies that CpdI is a weak base that cannot abstract a proton from ArgH$^+$.

$$ArgH^+ + CpdI \rightarrow Arg-H_a + FeOH^+ + 85.9 \text{ kcal mol}^{-1}$$

$$(6)$$

On the basis of the thermodynamic data of eq 5 and eq 6 it is clear that CpdI cannot react with ArgH$^+$ and, therefore, a more likely scenario is that ArgH$^+$ is deprotonated in an earlier step in the catalytic cycle. The catalytic cycle of NOS enzymes contains two protonation steps after dioxygen binding, namely protonation of the dioxo dianion (FeOO^{2-}) and of the hydroperoxo—iron complex (Cpd0). Thus, as follows from Figure 8, both the dioxo dianion and Cpd0 are more basic than arginine and are possible sources of proton abstraction from ArgH$^+$. Consequently, arginine will be deprotonated by the dioxo dianion quickly after its formation while the second proton in the catalytic cycle will originate from the solvent through a chain of water molecules that can relay the proton to the active site. This hypothesis is supported by studies of Davydov et al. and Couture et al. that implicated that arginine is deprotonated before hydroxylation takes place.[13] On the other hand, it has been suggested that the formation of the dioxo dianion follows a proton coupled electron transfer from the cofactor. If that hypothesis is correct, then ArgH$^+$ will donate the second proton in the catalytic cycle, that is, for the conversion of Cpd0 into CpdI. Nevertheless, the calculations support experimental work that the arginine substrate donates a proton in the catalytic cycle and will be in its neutral form in the reaction with the oxidant.

What is the Oxidant That Performs the Hydroxylation Reaction? To further establish whether CpdI or CpdII is the active oxidant of NOS enzymes, we calculated the electron affinity of CpdI (EA_{CpdI}) and the hydrogen abstraction energy (BDE_{OH}) of CpdI and CpdII. These values are shown in Figure 8 as well. The value of BDE_{OH} is similar to that defined above in eq 1 and relates to the energy difference of CpdI and an isolated hydrogen atom with the FeOH complex. The hydrogen abstraction energy (BDE_{OH}) of CpdI and CpdII are virtually the same (88.9 vs 86.4 kcal mol^{-1}) so that both species should be able to abstract a hydrogen atom from a substrate with equal probability. This is not surprising, since electronically CpdI and CpdII are the same except for a doubly occupied a_{2u} mixed thiolate/heme orbital in CpdII that is singly occupied in CpdI. The occupation of this orbital should not affect the hydrogen abstraction energies as indeed observed in Figure 8. The reaction energies of eq 7 and eq 8 for hydrogen abstraction of Arg$_a$ by CpdI and of Arg$_a^{+\bullet}$ by CpdII give almost equal reaction energies.

$$Arg_a^0 + CpdI \rightarrow Arg\text{-}H_{ab}^\bullet + FeOH^0 + 3.5 \text{ kcal mol}^{-1} \quad (7)$$

$$Arg_a^{+\bullet} + CpdII \rightarrow Arg\text{-}H_{ab}^+ + FeOH^{-1} + 0.3 \text{ kcal mol}^{-1} \quad (8)$$

Earlier theoretical studies on P450 enzymes and their hydroxylation mechanism of organic substrates showed that CpdI is the sole oxidant and no evidence of an alternative oxidant was found.[38] The reasons for the fact that here CpdII appears to be the active oxidant are that organic substrates have a high ionization potential, while the ionization energy of arginine is much lower. As a consequence, CpdI of NOS can take up an electron from arginine to form CpdII, whereas CpdI of P450 cannot abstract an electron from organic substrates due to their high ionization potentials. Since, CpdII has virtually the same oxidative power as CpdI, *cf.* Eq. 7 and 8, this has no further implications on the hydroxylation mechanism. Therefore, aliphatic C−H hydroxylation of organic substrates is performed by CpdI, whereas better ionizable substrates are hydroxylated by CpdII after reduction of CpdI to CpdII. In view of the fact that the substrates of P450 enzymes are mainly aliphatic systems these enzymes will react via CpdI and not via CpdII. It should be mentioned here that the QM/MM studies on the reactivity of P450 CpdI versus CpdII used the same substrate, namely camphor, and predicted the CpdII hydrogen abstraction barriers to be about 4 kcal mol^{-1} higher in energy than those observed for CpdI.[32b] By contrast, in this work the substrate donates an electron to CpdI and subsequently CpdII abstracts a hydrogen atom from the ionized substrate, which is a different comparison to that studied by Thiel et al. Since, hydrogen abstraction barriers correlate with the strength of the C−H bond in the substrate, BDE_{CH}, as well as with the newly formed O−H bond, BDE_{OH},[41] a difference in hydrogen abstraction barrier of 4 kcal mol^{-1} as observed by Thiel et al. implies that the BDE_{OH} of CpdI and CpdII are of the same order of magnitude as indeed observed in Figure 8.

Arginine, by contrast is a very special molecule with a very low ionization potential of 8.15 eV, and able to donate an electron to CpdI, especially in a polar environment where the positive charge is stabilized by a neighboring carboxylic acid group of Glu$_{363}$. Thus, the polar nature of the substrate binding pocket entices an electron abstraction by CpdI rather than a hydrogen abstraction and the formation of CpdII and an arginine cation radical. The latter is subsequently hydroxylated to form N^ω-hydroxo-arginine. Scheme 4 summarizes the main conclu-

sions on the basis of our DFT calculations. Thus starting from the dioxo-dianion species in the catalytic cycle of NOS, a fast proton abstraction from protonated arginine gives neutral arginine and Cpd0. This intermediate subsequently takes up a proton from a hydronium cation that via a chain of water molecules is connected to the surface of the enzyme. CpdI, once formed, abstracts an electron from neutral arginine to form CpdII and an arginine cation radical. CpdII is the active oxidant that abstract a hydrogen atom from arginine cation radical and a subsequent rebound of the hydroxo group gives N^ω-hydroxo-arginine products.

A Valence Bond Description of the Hydrogen Abstraction Reaction. Recently, a valence bond (VB) mechanism that describes the hydrogen abstraction reaction of aliphatic groups by CpdI of P450 enzymes has been devised.[42] Figure 9 shows the VB description as obtained for P450 on the left-hand side that represents the electronic transformations along the hydrogen abstraction coordinate via an intermediate with the metal in oxidation state Fe(IV). The heme is represented by two bold lines on the left and right-hand sides of the metal, and the substrate is abbreviated to R-H. In the reactant (CpdI), the high-lying occupied orbitals contain six π-electrons along the Fe−O bond with occupation $\pi_{xz}^2 \pi_{yz}^2 \pi^*_{xz}^1 \pi^*_{yz}^1$ and are represented by dots in Figure 9. Thus, the bonding and antibonding π and π^* orbitals along the Fe−O bond are occupied by six electrons and coupled into an overall triplet spin situation. In addition, CpdI has a third unpaired electron in a mixed thiolate/heme-type orbital (a_{2u}) to give the system the overall reactant wave function Ψ_r. Hydrogen abstraction by the oxo group leads to electron transfer from the substrate into this a_{2u} orbital but keeps the triplet situation in the π^* system to give the system the overall wave function Ψ_I(IV). The final step in the low-spin reaction mechanism leads to alcohol formation and the transfer of an electron into the π^* system to give the product complex and product wave function Ψ_p. The location of the transition states in the reaction mechanism are, therefore, dependent on the crossing points of the various wave functions shown in Figure 9. We showed with VB modeling that the height of the hydrogen abstraction barrier ($\Delta E^\ddagger$) can be expressed as a fraction (f) of the promotion gap (G_H), which represents the energy difference of Ψ_r and Ψ_I^* in the reactant geometry.[42] In addition, eq 9 contains a contribution for the resonance energy B.

$$\Delta E^\ddagger = f G_H - B \quad (9)$$

Thus, it was shown that the promotion gap includes 75% singlet to triplet excitation of the activated C−H bond of the substrate and as a consequence is correlated to the bond strength of the C−H bond, that is, BDE_{CH}.[43] Indeed, for a series of hydrogen abstraction reactions by CpdI of P450 enzymes, it was shown that the barrier heights correlated linearly with BDE_{CH}, in perfect agreement with the VB diagram shown in Figure 9a.[32a,42]

Using the same mechanism for the hydrogen abstraction of an N−H bond from protonated arginine in NOS enzymes (cf. Figure 2 above) rather than a C−H bond in the P450s, gives the same reaction profile with substrates as shown in Figure

(41) (a) Kaizer, J.; Klinker, E. J.; Oh, N. Y.; Rohde, J.-U.; Song, W. J.; Stubna, A.; Kim, J.; Münck, E.; Nam, W.; Que, L., Jr *J. Am. Chem. Soc.* **2004**, *126*, 472–473. (b) Mayer, J. M. *Acc. Chem. Res.* **1998**, *31*, 441–450.
(42) Shaik, S.; Kumar, D.; de Visser, S. P. *J. Am. Chem. Soc.* **2008**, *130*, 10128–10140.
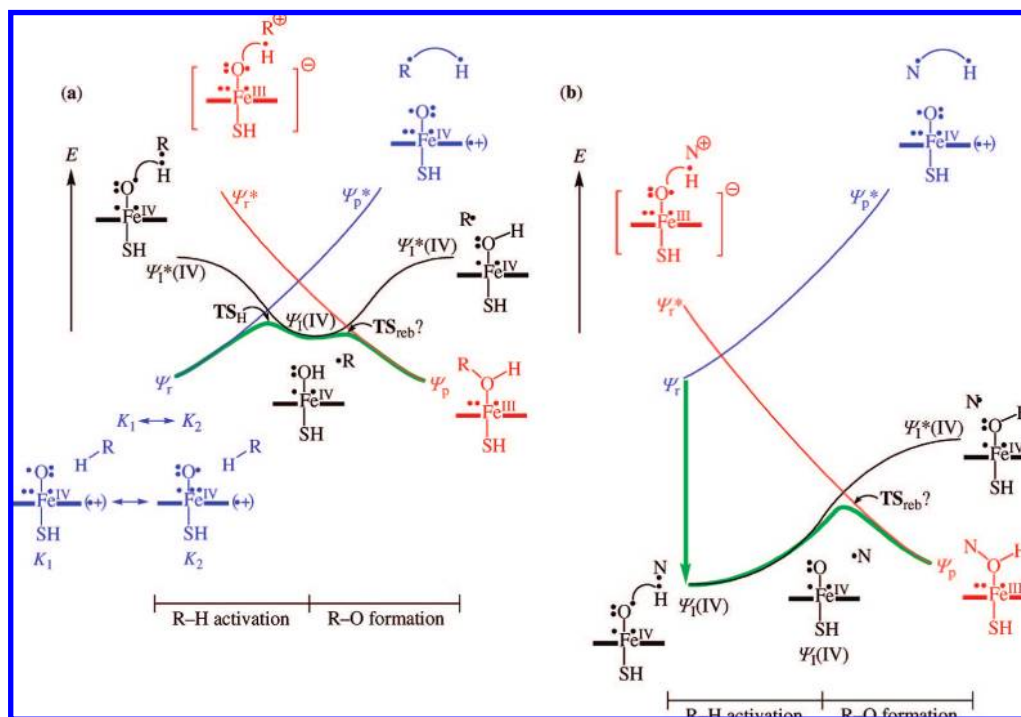(43) Shaik, S.; Shurki, A. *Angew. Chem., Int. Ed.* **1999**, *38*, 586–625.

Figure 9. Valence bond diagrams describing (a) the aliphatic C−H hydroxylation mechanism by CpdI of heme enzymes and (b) N−H hydroxylation by CpdII of NOS enzymes.

9a. Moreover, as shown in Figure 6 above, the BDE_{NH} of $ArgH^+$ is very high (112.1 kcal mol^{-1}), and as a consequence the hydrogen abstraction barrier is also very high (17.0 kcal mol^{-1} for $^4TS_{H,A}$). Similarly to C−H hydroxylation mechanisms discussed in the literature, also N−H hydroxylation of protonated arginine by CpdI proceeds via a stepwise mechanism on competing spin-state surfaces via multistate reactivity patterns as observed over and-over again for the P450s.[28−32,44] Therefore, the VB model shown in Figure 9a explains substrate hydroxylation of a C−H or N−H bond perfectly.

The situation for the deprotonated arginine model (CpdII$_B$) is slightly different. Thus, in these systems an electron transfer takes place prior to the hydrogen abstraction event to form CpdII and Arg$^{+•}$. In fact, what happens in those situations is schematically depicted in part b of Figure 9. Thus, in the reactant geometry an electron transfer takes place from a CpdI$_B$·Arg electronic situation (with wave function Ψ_r) to form CpdII$_B$·Arg$^{+•}$, and the system falls to the more stable $\Psi_I(IV)$ wave function. This contrasts the energy profile in Figure 9a, where the electron transfer from substrate to oxidant is endothermic, hence the $\Psi_I(IV)$ wave function is higher in energy than Ψ_r. This is because alkanes have a high ionization potential and the electron transfer reaction with CpdI to form CpdII and ionized alkane is endothermic, consequently the system will require energy to cross from reactants to the hydrogen abstraction intermediates with wave function $\Psi_I(IV)$. By contrast, neutral arginine has a low ionization potential and reacts with CpdI to form CpdII and Arg$^{+•}$ in an exothermic reaction. As a result of that, the wave function $\Psi_I(IV)$ is lower in energy than Ψ_r even in the reactant geometry so that the hydrogen abstraction reaction here is spontaneous, and only a rebound barrier separates reactants from products. The potential energy

profile for the low-spin state in Figure 4 supports this type of concerted mechanism, whereby only a single barrier has to be crossed on the way to products. Thus, the promotion gap G_H for the reaction displayed in Figure 9a reflects the energy difference between Ψ_r and $\Psi_I*(IV)$ in the reactant geometry, which essentially corresponds to the singlet−triplet energy gap for the R-H bond. This was shown to be proportional to BDE_{R-H},[43] so that the barrier height for the hydrogen abstraction is also linearly related to BDE_{R-H}. By contrast, in Figure 9b there is only one barrier for the reaction via the rebound transition state. As such, the promotion energy gap G_H in Figure 9b will correspond to the difference in energy of $\Psi_I(IV)$ and Ψ_r*, which is not proportional to the singlet−triplet energy gap for the N−H bond and as a consequence will also not be proportional to BDE_{N-H}. Instead the promotion gap in Figure 9b correlates with the electron transfer energy for the second electron transfer in the reaction, that is, from the substrate into the $\pi*_{xz}$ orbital.

The reaction profile for CpdII$_C$ also supports a mechanism shown in Figure 9b, where a negligible barrier separates the hydrogen abstraction intermediate from reactants. The efficiency of the oxidation reaction performed by CpdII is solely dependent on the rebound barrier in a pseudoconcerted reaction mechanism. In the case of the high-spin, the radical rebound encounters a significant barrier due to population of the $\sigma*_{z2}$ orbital with one electron, while in the low-spin a much lower lying $\pi*$ orbital is filled.[30a] As a consequence of this the reactivity of CpdII will take place on a dominant low-spin surface rather than on competing high-spin and low-spin surfaces with similar reaction barriers as usually observed.[32a] If this is a general paradigm than substrate oxidation of systems with a small ionization potential is expected to proceed via a mechanism as shown in Figure 9b where an initial electron transfer gives a CpdII-type

(44) (a) de Visser, S. P. *J. Phys. Chem. B* **2006**, *110*, 20759–20761. (b) de Visser, S. P. *J. Phys. Chem. B* **2007**, *111*, 12299–12302.

oxidant that reacts via a concerted reaction mechanism on a dominant low-spin surface with substrates.

Conclusion

In summary, DFT calculations on the catalytic cycle and substrate hydroxylation of NOS enzymes have established a new mechanism whereby the substrate acts first as a proton donor, then an electron donor and finally is hydroxylated. Thus, the calculations show that after dioxygen binding in the catalytic cycle an electron transfer gives the dioxo dianion complex. This complex picks up a proton from arginine to form compound 0, which takes a proton from the solvent (H_3O^+) to give CpdI. A fast electron transfer from the substrate to CpdI gives its one-electron reduced form CpdII and an arginine cation radical. The DFT calculations show that CpdII is the actual oxidant in NOS enzymes that performs the hydroxylation of arginine cation radical to give N^ω-hydroxo-arginine. These studies support experimental studies in the field that suggested that the substrate can donate a proton during the catalytic cycle.

Supporting Information Available: Complete ref 21; Cartesian coordinates of all structures described in this work, tables with group spin densities and charges, a figure with hydrogen abstraction energies from $Arg_d{}^0$. This material is available free of charge via the Internet at http://pubs.acs.org.

JA8010995